Title	Design of a droop control scheme for programmable sources in a microgrid testbed
Author(s)	Lim, Liang Yuan; Krishnan, Ashok; Foo, Eddy Yi Shyh
Citation	Lim, L. Y., Krishnan, A., & Foo, E. Y. S. (2018). Design of a droop control scheme for programmable sources in a microgrid testbed. IFAC-PapersOnLine, 51(28), 714-719. doi:10.1016/j.ifacol.2018.11.789
Date	2018
URL	http://hdl.handle.net/10220/47440
Rights	© IFAC 2018. This work is posted here by permission of IFAC for your personal use. Not for distribution. The original version was published in ifac-papersonline.net, DOI: [http://dx.doi.org/10.1016/j.ifacol.2018.11.789]

Available online at www.sciencedirect.com

ScienceDirect

IFAC Papers Online CONFERENCE PAPER ARCHIVE

IFAC PapersOnLine 51-28 (2018) 714–719

Design of a Droop Control Scheme for Programmable Sources in a Microgrid Testbed

Lim Liang Yuan * **Ashok Krishnan** * **Foo Y. S. Eddy** *

* *School of Electrical and Electronic Engineering, Nanyang Technological University, 50 Nanyang Avenue, Singapore 639798. (e-mail: E150095@e.ntu.edu.sg).*

Abstract: The Clean Energy Research Lab (CERL) in Nanyang Technological University, Singapore has a three-phase, 400V, 50Hz microgrid (MG) testbed to perform power system studies. The MG testbed comprises a 13.5kVA synchronous generator, 18kVA programmable source, 6kvar capacitor bank, 5kW solar photovoltaic (PV) system, 13.5kW wind simulator, 5kW battery energy storage system (BESS), 5kW fuel cell, 13.5kW programmable load as well as a 10kW simulated industrial load. The MG can operate either in islanded mode or in grid-connected mode. In the islanded mode, distributed generators such as the synchronous generator and the programmable source determine the frequency and voltage of the MG. A major difference between the synchronous generator and the programmable source is that the synchronous generator has inertia while the programmable source is inertialess. This means that the former has an inherent power-frequency droop associated with it whereby the synchronous generator frequency changes according to its power generated. Conversely, the programmable source does not have a power-frequency droop characteristic since it has no rotating parts. This paper demonstrates how the programmable source can be programmed to contain the power-frequency droop characteristics inherent to the synchronous generator. The experimental results presented in this paper are obtained from the CERL MG testbed. The results demonstrate the utility and performance of the developed droop scheme.

Keywords: Electric power systems, Hardware, Load frequency control, Renewable energy systems, Solar energy, Synchronous machines, Virtual inertia.

1. INTRODUCTION

In an electric power system, the generation and demand must be in equilibrium at all times. Day-ahead load forecasts are used to optimally commit and schedule generators using advanced optimization techniques. Growing environmental concerns in recent years have led to an increase in the use of renewable energy sources. The Energy Market Authority (EMA) of Singapore reported an increase in the total installed capacity of solar power from 278.7kW in 2008 to 108,834kW in 2017 [EMA (2017)]. The introduction of distributed generators such as solar PV power plants to the grid has posed several new challenges to the system planners. In this context, many researchers have been focusing on strategies to operate renewable energy inverters in both grid-connected and islanded modes. It is evident that modern renewable energy inverters need to be adept at switching between the grid-connected and islanded modes of operation [Vasquez et al. (2009), Kulkarni et al. (2016)]. Furthermore, the intermittent nature of the renewable energy sources coupled with the presence of inertialess power electronic converters could lead to grid stability issues. A recent review paper highlighted the need to simplify algorithms used in controlling the MG [Han et al. (2017)]. Predictive control based approaches have also gained popularity in recent years [Han et al. (2017)]. Reactive power sharing between subsystems within a MG to improve stability has also been an active research area [Han et al. (2017)].

To mitigate some of the issues caused by the intermittent RESs, many researchers have been studying ways to add inertia to the MG to improve its stability [Soni et al. (2013)]. The impact of intermittent RESs is more pronounced on islanded MGs which have no rotating machines to provide inertia to stabilize the system [Kerdphol et al. (2017)]. One way to mitigate this issue is to introduce virtual inertia in the system [Wang et al. (2017a)]. In addition to this, several other approaches have been proposed in the literature. The authors of Wang et al. (2017b) proposed the addition of a virtual impedance to balance the differences in feeder impedance. The dynamic responses of virtual synchronous generators and inverter droops have been simulated to study the effects of large scale renewable energy integration with the main grid [Liu et al. (2016)]. Hardware implementations have also recently attracted research attention. Many recent works introduced inertia to virtual synchronous machines using AC-DC links in a MG. DC storage devices are often required in the grid to simulate the virtual inertia along with their associated power electronic converters [Ma et al. (2015); Fang et al. (2017)].

10.1016/j.ifacol.2018.11.789

This paper examines the feasibility of conducting hardware experiments with programmable devices in a laboratory-based MG testbed. The droop characteristics and inertia of a synchronous generator are programmed on a three-phase AC programmable source. Tests are conducted to study the interactions between the programmable source and an actual synchronous generator. This setup could potentially reduce the need for excessive hardware requirements to test new theories and algorithms, thereby enabling faster prototyping of research projects.

The remainder of this paper is organized as follows: Section 2 describes some theoretical background to the experiments conducted in this paper; Section 3 describes the MG testbed equipment used for the experiments in this paper; Section 4 presents the results of the hardware experiments performed on the MG testbed and Section 5 concludes the paper.

2. THEORETICAL BACKGROUND

The frequency and speed of a rotor are correlated using the following equation:

$$f = n_s p/120 \tag{1}$$

where f represents the frequency; n_s represents the rotor speed in rpm and p represents the number of poles in the stator.

The droop of a single generator is modelled using the straight-line equation:

$$y = mx + c \tag{2}$$

where y represents the rotor speed of the generator in rpm or the frequency in Hz; x represents the power delivered by the generator in W; m represents the gradient of the droop and c represents the no-load speed of the rotor in rpm or the no-load frequency in Hz.

Initially, simulation studies were performed using LabVIEW to study the interactions between 2 generators in the MG. To prevent any competition between the 2 generators to perform the load frequency control (LFC) action, the controller was programmed to ensure that only one generator had LFC enabled at any time instant. However, if either generator reached its maximum capacity limit, the LFC action was disabled to prevent any overcapacity related issues. Concurrently, if the other generator was still operating within its capacity limits, it was allowed to control the system frequency. The loads were divided among the two generators in a random fashion without formulating any economic dispatch problem. The capacities of the 2 generators in the simulation study were 1kW and 1.5kW respectively. Fig 1 illustrates the results of the simulation study. Fig. 1 depicts a scenario wherein most of the load demand is assigned to Generator 2 while only a small amount of load is assigned to Generator 1. The system frequency is maintained at 50Hz in Fig. 1.

3. MICROGRID TESTBED EQUIPMENT

3.1 Chroma Programmable AC Source 61512

The Chroma Programmable AC Source shown in Fig. 2 is an 18kVA power supply which delivers a pure AC sine wave at the designated frequency. It is an inertialess

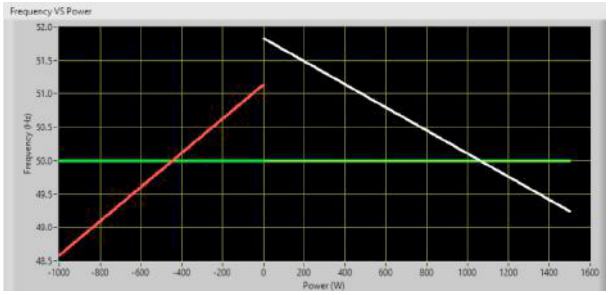

Fig. 1. Multiple generator droop curve simulation using LabVIEW

source which derives its power electronically from power converters. The droop is assigned to the programmable source through LabVIEW using the TCP/IP protocol. The following equation is used to define the linear relationship between the output power produced by the programmable source and the frequency:

$$y = -1.389\text{e}^{-4}x_{\text{ps}} + c \tag{3}$$

where x_{ps} represents the power delivered by the programmable source in W which is closely monitored by smart meters in the MG and c is kept at 50Hz when there is no LFC action. For each iteration, the new frequency values are determined proportional to the power output. When the LFC action is enabled, the value of c is altered. Subsequently, the LabVIEW algorithm recalculates the corresponding frequency, thereby ensuring that the programmable source displays the characteristics of a droop similar to a synchronous generator.

Fig. 2. Image of Chroma Programmable AC Source 61512

3.2 Synchronous Generator

The synchronous generator used in the hardware setup for this paper is a 13.5kVA Marelli Generator with 4 poles as shown in Fig. 4. The generator operates at 1500rpm, 50Hz. The synchronous generator is mechanically coupled with an induction motor which performs the role of a prime mover. Unlike the programmable source, the droop equation is inherent to the synchronous generator and cannot be altered. The droop curve inherent to the synchronous generator is determined experimentally and is shown below in Fig. 3. The droop equation extracted from Fig. 3 is shown in (4). The droop equation shown in (4) has been used in all the experimental studies performed in this paper.

$$\bar{y} = -3.9707\text{e}^{-3}x_{\text{sg}} + \bar{c} \tag{4}$$

where $\bar{y}$ represents the rotor speed of the synchronous generator in rpm; x_{sg} represents the power produced by

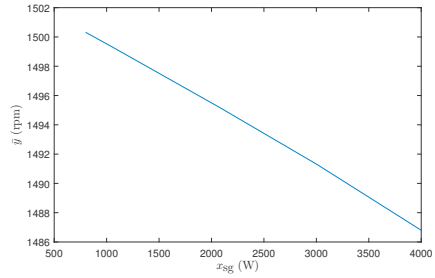

Fig. 3. Experimentally determined droop curve of the synchronous generator

Fig. 4. Image of 13.5kVA, 4 pole, Marelli Generator

the synchronous generator in W or kW and $\bar{c}$ represents the no-load speed of the synchronous generator in rpm.

The load demand in the microgrid was divided between the synchronous generator and the programmable source in the same proportion as their respective maximum capacities. Consequently, approximately 42.9% of the total load was allocated to the synchronous generator. The no-load speed setting of the synchronous generator was adjusted according to the following equation:

$$\bar{c} = 3.9707\text{e}^{-3} x_{\text{tot}} k + 1500 \tag{5}$$

where x_{tot} represents the total power generated at any time instant by the programmable source and the synchronous generator and k represents the load sharing factor.

3.3 Chroma Programmable AC/DC Electronic Load 63800

The Chroma Programmable Load shown in Fig. 5 is used to introduce dynamic loads into the system. The programmable load can be varied with a high degree of accuracy as opposed to variable manual loads which are unable to achieve consistent loading levels. The Chroma Programmable Load is capable of operating in several modes. For the studies performed in this paper, the Chroma Programmable Load was operated in the constant power (CP) mode.

4. RESULTS

4.1 Standalone Operation

In the first scenario, the programmable source is operated in standalone mode and the performance of the programmed generator droop characteristic is verified. In Fig.

Fig. 5. Image of Chroma Programmable AC/DC Electronic Load 63800

6, it is observed that the no-load speed setting increases from the initial 50Hz to 50.5Hz in order to supply 4kW of load at 50Hz system frequency. The red line represents the system frequency while the blue line represents the corresponding power delivered by the programmable source. The green line represents the initial droop position before the LFC action is enabled wherein the no-load speed setting is 50Hz.

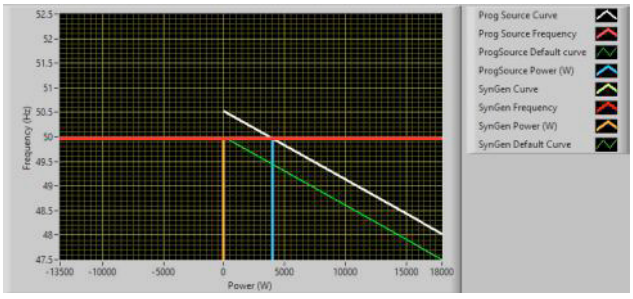

Fig. 6. Programmable source programmed with droop curves delivering 4kW of load before and after enabling LFC action

4.2 Parallel operation of two generators

Fig. 7 shows how the synchronous generator and programmable source behave when they are deployed together on the same grid. In this scenario, the LFC action is executed by the programmable source. The power flow between the generators can be adjusted manually by adjusting the no-load setpoint. It is observed that the programmable source does not act as an infinite bus. The droop characteristics of a generator are clearly exhibited by the programmable source. The interaction between the synchronous generator and the programmable source clearly resembles the droop interaction usually observed between two synchronous generators. Minor frequency adjustments are observed during the live operation of the system. This is due to the fluctuating system frequency measurements obtained from the smart meters. There is often a dead band to which the LFC action does not respond [Kundur et al. (1994)].

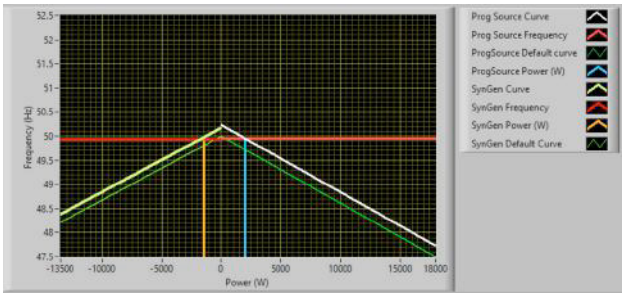

Fig. 7. Synchronous generator and programmable source sharing a total load of 3.5kW

4.3 Implementation of Inertia

Due to the absence of any rotor and stator interactions, parameters such as inertia and oscillation damping are not relevant for the programmable source. The impact of a lack of inertia in the system can be seen when the system frequency changes rapidly due to a sudden load change. Due to the lack of inertia, the rate of change of frequency (ROCOF) is high when there is a large increase in the load. The system frequency fluctuation is extremely responsive to the LFC action. The ROCOF of a typical synchronous generator can be described using the following equation:

$$M\frac{d\omega}{dt} = P_m - P_e = P_a \tag{6}$$

where M represents the inertia constant of the generator (MJ-s/electrical rad); ω represents the rotor speed (rpm or Hz); t represents time (s); P_m represents the mechanical power (kW) and P_e represents the electrical power (kW).

The droop equation determines the amount of frequency change that occurs when the system load changes. However, the rate of frequency change is dependent on the swing equation described in (6). For an inertialess generator, P_m is used to express the programmable source no-load speed setting in terms of power and P_e is the power delivered to the grid by the programmable source. When the system frequency deviates from the nominal frequency, the swing equation should calculate the trajectory of the rate of change in frequency to reach the frequency setpoint determined by the droop equation. Figs. 8 and 9 show how the grid frequency responds when inertia is introduced in the system.

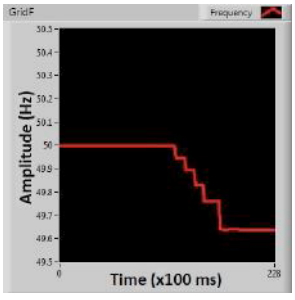

Fig. 8. Grid frequency without inertia using the programmable source

Fig. 8 shows how the grid frequency responds to a load change of 2.6kW without any inertia. The grid Frequency is observed to drop rapidly to 49.6Hz from the initial 50Hz.

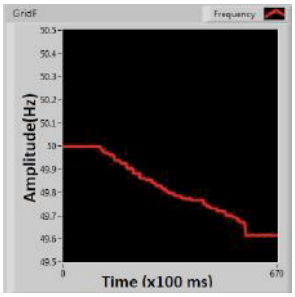

Fig. 9. Grid frequency with inertia using the programmable source

Fig. 9 shows the trajectory of the system frequency when an inertia constant of 105 is introduced. The time taken for the source to reach the required frequency setpoint is longer due to the introduction of the inertia. Further analysis of the ROCOF can be derived from examining the ROCOF curves as shown below.

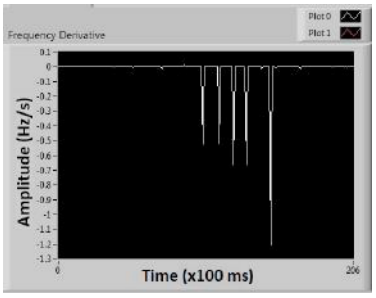

Fig. 10. Rate of change of frequency with no inertia

It is observed that the smart meters record 5 instances of rapid frequency changes as shown in Fig. 10. The sampling time of the smart meters is 1s. The peak value of ROCOF was recorded at around -1.2Hz/s which is quite high. The programmable source took 5 setpoints to reach the final grid frequency of 49.6Hz.

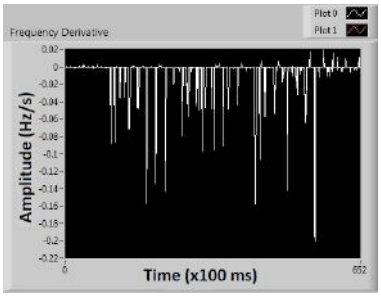

Fig. 11. Rate of change of frequency with inertia

The value of ROCOF is significantly lower when inertia is introduced in the system. The peak value was recorded to be around -0.2Hz/s. The programmable source takes several setpoints to approach the final grid frequency of 49.6Hz. This allows the trajectory of the grid frequency to be smoother, thereby simulating the effect of a system with high inertia.

4.4 Load Frequency Control

In the existing system, the LFC parameter is tuned to adjust progressively while correcting frequency deviations

in the grid. This is to prevent overcorrection and system instability when there is a deviation in grid frequency. The modified LFC equation for the programmable source is shown below.

$$y = (-1.389\mathrm{e}^{-4}x)K + c \tag{7}$$

A K value of 0.25 is used in the system. This variable is tuned after running several tests on the system. Without this variable, the system is unable to attain stability after correcting from a frequency deviation. A lack of oscillation causes further instability when a major frequency deviation occurs in the system.

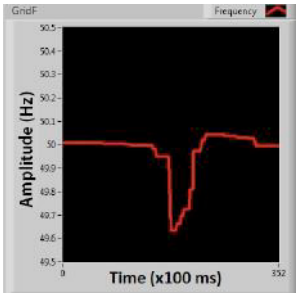

Fig. 12. Load frequency control (Stable)

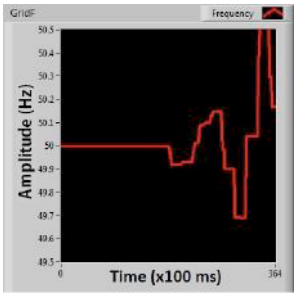

Fig. 13. Load frequency control (Unstable)

In Fig. 12, a 2.6kW load is added to an existing 0.6kW load. The programmable source is able to restore the grid frequency back to 50Hz with the implementation of the LFC algorithm. The LFC action was tuned with K=0.25, thereby allowing for a progressive corrective action. This causes the frequency to take a longer time to settle back to 50Hz. However, the stability of the grid is ensured in the process. In Fig. 13, a load of 0.6kW is added to the grid. The LFC action was implemented with K=1. In this scenario, the corrective action from the LFC algorithm is immediate. This leads to an overcorrection which consequently results in a divergent trajectory for the grid frequency, thereby making the system unstable.

5. CONCLUSION

Further improvements could be made to the setup by including more constraints on the programmable source. This would allow the programmable source to have a realistic performance when compared with actual synchronous machines. Despite the obvious room for improvement, the current setup clearly demonstrates the versatility of a programmable source in providing rapid prototyping and testing capabilities for a MG testbed. This could aid future researchers in testing new theories and algorithms on a MG testbed in a short period of time. The full potential of the setup demonstrated in this paper is yet to be explored. An interesting direction for future work would be to emulate and program the action of the synchronous generator damper windings in the programmable source. The authors also plan to develop a simulation model of the MG and compare the simulation results with the experimental results obtained from the MG testbed.

ACKNOWLEDGEMENTS

The authors would like to acknowledge the funding support from NTU Set-Up Grant.

REFERENCES

EMA (2017). *Singapore Energy Statistics 2017*. Energy Market Authority, Singapore.

Fang, J., Li, X., and Tang, Y. (2017). Grid-connected power converters with distributed virtual power system inertia. In *2017 IEEE Energy Conversion Congress and Exposition (ECCE)*, 4267–4273.

Han, Y., Li, H., Shen, P., Coelho, E.A.A., and Guerrero, J.M. (2017). Review of active and reactive power sharing strategies in hierarchical controlled microgrids. *IEEE Transactions on Power Electronics*, 32(3), 2427–2451.

Kerdphol, T., Rahman, F.S., Mitani, Y., Watanabe, M., and Kfeolu, S. (2017). Robust virtual inertia control of an islanded microgrid considering high penetration of renewable energy. *IEEE Access*, PP(99), 1–1.

Kulkarni, O.V., Doolla, S., and Fernandes, B.G. (2016). Mode transition control strategy for multiple inverter based distributed generators operating in grid-connected and stand-alone mode. In *2016 IEEE Applied Power Electronics Conference and Exposition (APEC)*, 3376–3382.

Kundur, P., Balu, N.J., and Lauby, M.G. (1994). *Power system stability and control*, volume 7. McGraw-hill New York.

Liu, J., Miura, Y., and Ise, T. (2016). Comparison of dynamic characteristics between virtual synchronous generator and droop control in inverter-based distributed generators. *IEEE Transactions on Power Electronics*, 31(5), 3600–3611.

Ma, T., Cintuglu, M.H., and Mohammed, O. (2015). Control of hybrid ac/dc microgrid involving energy storage, renewable energy and pulsed loads. In *2015 IEEE Industry Applications Society Annual Meeting*, 1–8.

Soni, N., Doolla, S., and Chandorkar, M.C. (2013). Improvement of transient response in microgrids using virtual inertia. *IEEE Transactions on Power Delivery*, 28(3), 1830–1838.

Vasquez, J.C., Guerrero, J.M., Luna, A., Rodriguez, P., and Teodorescu, R. (2009). Adaptive droop control applied to voltage-source inverters operating in grid-connected and islanded modes. *IEEE Transactions on Industrial Electronics*, 56(10), 4088–4096.

Wang, C., Meng, J., Wang, Y., and Wang, H. (2017a). Adaptive virtual inertia control for dc microgrid with variable droop coefficient. In *2017 20th International Conference on Electrical Machines and Systems (ICEMS)*, 1–5.

Wang, W., Wang, Y., Li, M., Xu, N., and Li, Z. (2017b). A novel transient power control strategy for inverters in

voltage control mode. In *2017 IEEE 3rd International Future Energy Electronics Conference and ECCE Asia (IFEEC 2017 - ECCE Asia)*, 1591–1595.